

Projections for Neutral Di-Boson and Di-Higgs Interactions at FCC-he Collider

S. Kuday,^{*} H. Saygin,[†] İ. Hoş,[‡] and F. Çetin[§]

*Istanbul Aydın University, Application and Research
Center For Advanced Studies, 34295, Istanbul, Turkey*

Abstract

As a high energy e-p collider, FCC-he, has been recently proposed with sufficient energy options to investigate Higgs couplings. To analyse the sensitivity on Higgs boson couplings, we focus specifically on the CP-even and CP-odd Wilson coefficients with $hhZZ$ and $hh\gamma\gamma$ four-point interactions of Higgs boson with Effective Lagrangian Model through the process $e^-p \rightarrow hhje^-$. We simulate the related processes in FCC-he, with 60 GeV and 120 GeV e^- beams and 50 TeV proton beam collisions. We present the exclusion limits on these couplings both for 68% and 95% C.L. in terms of integrated luminosities.

^{*} sinankuday@aydin.edu.tr

[†] hasansaygin@aydin.edu.tr

[‡] ilknurhos@aydin.edu.tr

[§] fusuncetin@aydin.edu.tr

I. INTRODUCTION

The discovery of the Higgs boson [1, 2] and the consistency of Higgs measurements by ATLAS and CMS [3, 4] brought up all available Higgs production and decay channels to an utmost importance level. Of these channels, arguably the most important ones are the Higgs-self coupling (λ) and the anomalous couplings, since it will show a direct evidence of the Electroweak Symmetry Breaking (EWSB) mechanism [5] which is expected to work as predicted by Standard Model (SM).

Over the years, extensive studies have shown that it is quite challenging to observe the Yukawa couplings of Higgs boson to other fermions even with the correction algorithms at the LHC through gluon-fusion process due to the enormous SM background [6]. Although Vector Boson Fusion (VBF) processes are accesible at the LHC [7], there are studies suggest that it is more feasible to accomplish this task using linear colliders [8] or through ep-collisions [9]. Consequently, searching for Higgs decays at future colliders became relatively important just because they bring unique opportunities to fully cover SM scalar sector [10]. To study anomalous couplings, di-Higgs boson production through charged current (CC) mechanisms are well studied in Large Hadron Electron Collider (LHeC) and Future Circular Collider (FCC-he) [11] expressing that neutral current (NC) mechanisms have a potential to enhance the overall Higgs boson signal efficiency. In addition, for the completeness of the studies based on the Higgs Effective Lagrangian Model [14], it is quite promising to study on di-higgs productions via four-point interaction vertices since it contains aspects for both new physics and SM Higgs studies. However a complete understanding of Higgs sector can open doors to new physics and particles. Likewise, it has recently been reported that if additional scalar bosons exist, they can be interpreted in the effective theory approach leaving signatures in the final states with a pair of invisible χ particles that are proposed to be the dark matter candidate [15]. According to this approach, newly proposed heavy Higgs boson eventually decays to a Higgs boson and a pair of χ , causing a distortion in the p_T distribution that are compatible with the observations at LHC [16].

Here, it is considered the electron - proton collision variant of the FCC-he that is proposed to build on the same site with LHC, as the future extension of the LHeC. In FCC-he, construction of an Energy Recovery Linac is proposed to deliver electrons with energies ranging from $E_e = 60 \text{ GeV}$ to $E_e = 120 \text{ GeV}$, while a proton beam is provided by a 100 km

circular beam pipe and has an maximum proton energy of $E_p = 50 \text{ TeV}$.

The main idea in this letter is that by analysing neutral four-point interactions in FCC-he, one can get rid of a part of the SM background and get a better detection efficiency by electron tracks involved in the final state which can be reconstructed efficiently. We studied Higgs boson couplings at neutral four-point interaction vertices through Wilson coefficients within the Higgs Effective Lagrangian Model. The outline of our paper has been prepared as in the following: In section 2, we basically reveal the related Lagrangian terms and their phenomenological interpretations as well as the assumptions of our case. In section 3 and 4, we discuss event productions for signal and background processes respectively. In section 5, we explain applied event selection criterias and statistical analysis of data that we obtained from simulation tools. Finally in section 5, we present our results and exclusion limits for obtaining related coefficients in FCC-he collisions.

II. HIGGS EFFECTIVE LAGRANGIAN (HEL) MODEL

Since the details of the Higgs sector is not trivial, an effective field theory (EFT) that covers all related interactions at a given scale, but not the others that play a role at significantly different scales, might be a good approach. In EFT models, particularly interactions at much higher energies than the energy scale of interest are ignored. So that the underlying physics event at energies below the new physics scale can be described precisely. In this letter, we studied on the exclusive Higgs Effective Lagrangian (HEL) Model, that is valid above a Λ scale around TeV order, makes possible to include dimension-six operators with free parameters, namely, Higgs self-couplings, Yukawa couplings and Wilson coefficients. In this approach, the complete Lagrangian is handled by SM Lagrangian and supplemented higher dimensional operators which are assumed to appear at energies larger than the effective scale. \mathcal{L} , the most general gauge-invariant total Lagrangian, can be expressed as in the followings with Wilson coefficients \bar{c}_i and independent operators \mathcal{O}_i of dimension less than or equal to six.

$$\mathcal{L} = \mathcal{L}_{SM} + \sum_i \bar{c}_i \mathcal{O}_i = \mathcal{L}_{SM} + \mathcal{L}_{SILH} + \mathcal{L}_{CPV} + \dots \quad (1)$$

After EWSB, the Higgs sector can be expressed as;

$$\mathcal{L}_{Higgs} = \mathcal{L}^{(3)} + \mathcal{L}^{(4)} + \mathcal{L}^{(5)} + \mathcal{L}^{(6)} \quad (2)$$

where numbers in superscript denotes the set of interactions of a Higgs boson with a vector boson pair. Related Lagrangians can specifically be rewritten as follows for the mass basis.

$$\mathcal{L}_{hhh}^{(3)} = -\frac{m_H^2}{2v} g_{hhh}^{(1)} h^3 + \frac{1}{2} g_{hhh}^{(2)} h \partial_\mu h \partial^\mu h \quad (3)$$

$$\mathcal{L}_{hzz}^{(3)} = -\frac{1}{4} g_{hzz}^{(1)} Z_{\mu\nu} Z^{\mu\nu} h - g_{hzz}^{(2)} Z_\nu \partial_\mu Z^{\mu\nu} h + \frac{1}{2} g_{hzz}^{(3)} Z_\mu Z^\mu h - \frac{1}{4} \tilde{g}_{hzz} Z_{\mu\nu} \tilde{Z}^{\mu\nu} h \quad (4)$$

$$\mathcal{L}_{h\gamma\gamma}^{(3)} = -\frac{1}{4} g_{h\gamma\gamma} F_{\mu\nu} F^{\mu\nu} h - \frac{1}{4} \tilde{g}_{h\gamma\gamma} F_{\mu\nu} \tilde{F}^{\mu\nu} h \quad (5)$$

$$\mathcal{L}_{hhzz}^{(4)} = -\frac{1}{8} g_{hhzz}^{(1)} Z_{\mu\nu} Z^{\mu\nu} h^2 - \frac{1}{2} g_{hhzz}^{(2)} Z_\nu \partial_\mu Z^{\mu\nu} h^2 + \frac{1}{4} g_{hhzz}^{(3)} Z_\mu Z^\mu h^2 - \frac{1}{8} \tilde{g}_{hhzz} Z_{\mu\nu} \tilde{Z}^{\mu\nu} h^2 \quad (6)$$

$$\mathcal{L}_{hh\gamma\gamma}^{(4)} = -\frac{1}{8} g_{hh\gamma\gamma} F_{\mu\nu} F^{\mu\nu} h^2 - \frac{1}{8} \tilde{g}_{hh\gamma\gamma} F_{\mu\nu} \tilde{F}^{\mu\nu} h^2 \quad (7)$$

Here, tilde operator denotes the CP-violating terms, while all other non-tilde terms are CP-conserving. One can also consider other neutral four-point interactions such as di-higgs and di-gluon or quartic-self-interaction of Higgs. But these processes are shown to give no events at FCC-he collider. Therefore we can describe the general Lagrangian that we are working on as $\mathcal{L} = \mathcal{L}_{\mathcal{SM}} + \mathcal{L}_{hhh}^{(3)} + \mathcal{L}_{hzz}^{(3)} + \mathcal{L}_{h\gamma\gamma}^{(3)} + \mathcal{L}_{hhzz}^{(4)} + \mathcal{L}_{hh\gamma\gamma}^{(4)}$. Several different representations of couplings in Eq. (3-7) are available via FCNC notation [17]. In principle, we concentrate on gauge basis representations of couplings with Wilson coefficients as in Table 1 - 2 and take the same notation as explicitly described in [19]. From Table 2, one can see that $g_{hh\gamma\gamma}$ ($\tilde{g}_{hh\gamma\gamma}$) strictly corresponds to terms with only \bar{c}_γ (\tilde{c}_γ) coefficient, while g_{hhzz} (\tilde{g}_{hhzz}) indirectly corresponds to terms with coefficients $\bar{c}_{HB}, \bar{c}_{HW}, \bar{c}_\gamma, \bar{c}_W$ ($\tilde{c}_{HB}, \tilde{c}_{HW}, \tilde{c}_\gamma, \tilde{c}_W$) for the first two orders, respectively. And for the third order of g_{hhzz} , it is seen an explicit dependence to $\bar{c}_T, \bar{c}_H, \bar{c}_\gamma$. To scan over these parameters, we explain our strategy in the next section with the case-specific assumptions. To understand physical analysis of EFT explicitly, one must build SILH (Strongly-Interacting Light Higgs) Lagrangian in terms of indepent operators as shown in Eq. (1) and described in Ref [18]. One can then discuss the relative effect of

Table I: Corresponding couplings of a Higgs boson and a pair of neutral bosons in the mass and gauge basis for Eq. (3) as in Ref [14].

Mass Basis	Gauge Basis
$g_{hhh}^{(1)}$	$1 + \frac{7}{8}\bar{c}_6 - \frac{1}{2}\bar{c}_H$
$g_{hhh}^{(2)}$	$\frac{g}{m_W}\bar{c}_H$
$g_{h\gamma\gamma}$	$a_H - \frac{8g\bar{c}_\gamma s_W^2}{m_W}$
$\tilde{g}_{h\gamma\gamma}$	$-\frac{8g\bar{c}_\gamma s_W^2}{m_W}$
$g_{hzz}^{(1)}$	$\frac{2g}{c_W^2 m_W}[\bar{c}_{HB}s_W^2 - 4\bar{c}_\gamma s_W^4 + c_W^2\bar{c}_{HW}]$
$g_{hzz}^{(2)}$	$\frac{g}{c_W^2 m_W}[(\bar{c}_{HW} + \bar{c}_W)c_W^2 + (\bar{c}_B + \bar{c}_{HB})s_W^2]$
$g_{hzz}^{(3)}$	$\frac{gm_W}{c_W^2}[1 - \frac{1}{2}\bar{c}_H - 2\bar{c}_T + 8\bar{c}_\gamma \frac{s_W^4}{c_W^2}]$
\tilde{g}_{hzz}	$\frac{2g}{c_W^2 m_W}[\tilde{c}_{HB}s_W^2 - 4\tilde{c}_\gamma s_W^4 + c_W^2\tilde{c}_{HW}]$

Table II: Corresponding couplings of Higgs and neutral boson pairs in the mass and gauge basis for Eq. (3) as in Ref [14].

Mass Basis	$g_{hh\gamma\gamma}$	$\tilde{g}_{hh\gamma\gamma}, \tilde{g}_{hhzz}$	$g_{hhzz}^{(1)}, g_{hhzz}^{(2)}$	$g_{hhzz}^{(3)}$
Gauge Basis	$-\frac{4\bar{c}_\gamma g^2 s_W^2}{m_W^2}$	$\frac{g}{2m_W}\{\tilde{g}_{h\gamma\gamma}, \tilde{g}_{hzz}\}$	$\frac{g}{2m_W}\{g_{hzz}^{(1)}, g_{hzz}^{(2)}\}$	$\frac{g^2}{2c_W^2}[1 - 6\bar{c}_T - \bar{c}_H + 8\bar{c}_\gamma \frac{s_W^4}{c_W^2}]$

the various operators on physical observables through Wilson coefficients. However, SILH Lagrangian includes only CP-conserving operators multiplied with Higgs related fields. For completeness, one should also add a CP-violating Lagrangian as in Eq. (1) which has the same interactions with SILH Lagrangian but rewritten with CP-violating coefficients ($\tilde{c}_{HB}, \tilde{c}_{HW}, \tilde{c}_\gamma, \tilde{c}_W$) and operators. One of the naive ways of estimating these coefficient values has been made by power counting after expanding the effective Lagrangian in the number of fields and derivatives at tree level. According to power counting for the related terms that we are interested in, one can estimates;

$$\bar{c}_6, \bar{c}_H, \bar{c}_T \sim O\left(\frac{v^2}{f^2}\right) \quad \bar{c}_W, \bar{c}_B \sim O\left(\frac{m_W^2}{M^2}\right) \quad \bar{c}_{HB}, \bar{c}_{HW}, \bar{c}_\gamma, \bar{c}_g \sim O\left(\frac{m_W^2}{f^2}\right) \quad (8)$$

where v is vacuum expectation value, f denotes the coupling strength of the Higgs boson to New Physics states and M is the overall mass scale. If one defines the new physics coupling as g_{NP} , f can explicitly be written as g_{NP}/M . Above the tree level, related coefficient will be shifted upper values slightly getting contributions from extra terms depend on the mass scale, M . Although we shall comment on these effects in the conclusion, it should be noted that the further evaluations and analysis on the topic are beyond the scope of this letter.

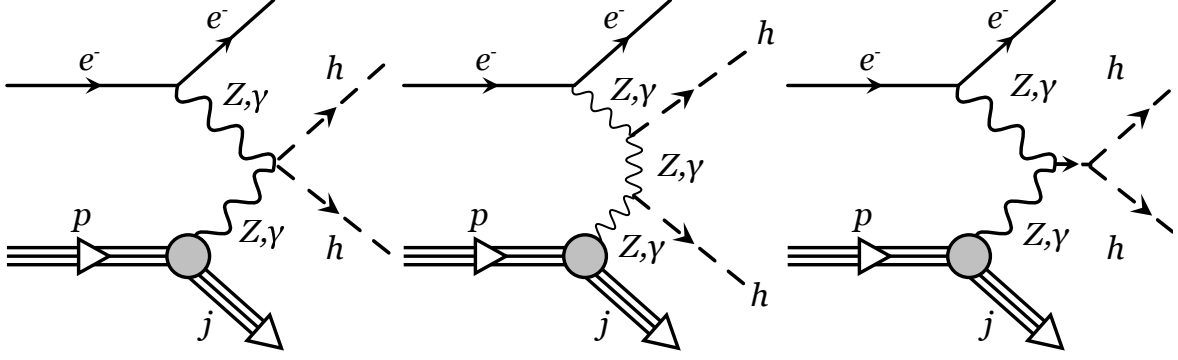


Figure 1: Feynman Diagrams for the signal processes

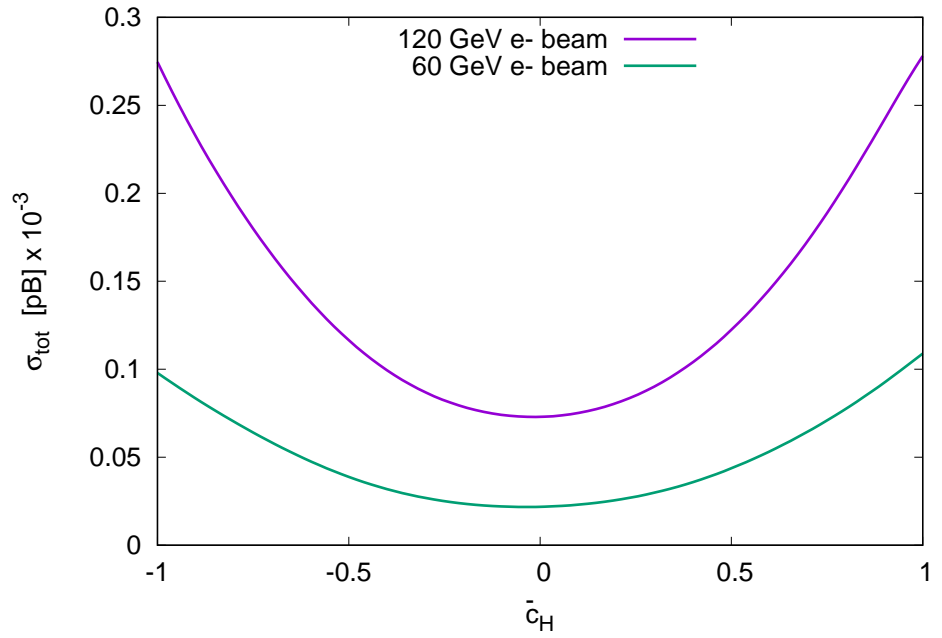
III. SIGNAL PRODUCTION

For signal production, we have used the implementation of a Higgs Effective Field Theory in MadGraph5 Model [20] with FeynRules [21] that is available including full lagrangian terms and a set of independent dimension-six operators. As shown in Fig.1, we produced events of $e^-p \rightarrow hhje^-$ processes using HEL model taking into account effective vertices and keeping e-p collider set up at $\sqrt{s} \approx 3.5 \text{ TeV}$ and $\sqrt{s} \approx 5 \text{ TeV}$ which are the two main options of FCC-he.

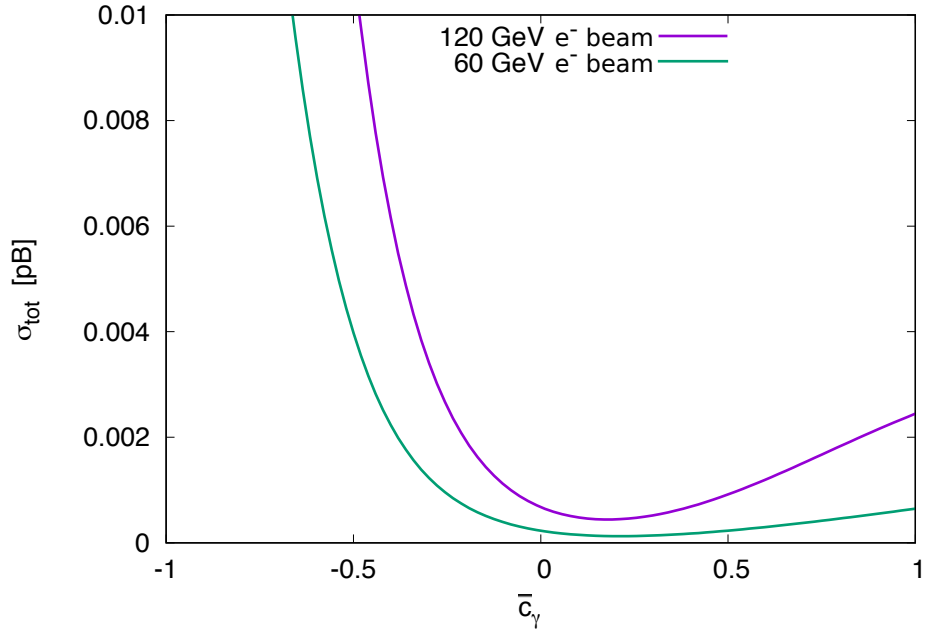
Here, we are searching for both Z bosons and γ as mediators that together forms the NC processes. One can name each subprocesses as Vector Boson Fusion (VBF) with Z boson and photo fusion (PF) with γ mediators, respectively. Due to gauge invariant structure of HEL model, one can not actually separate event productions for Z boson and γ mediators. However, it is possible to minimize the contribution of one of the subprocesses setting related Wilson coefficients as below. The corresponding couplings of PF process are well known with already studied in letters Ref [12, 13] for different colliders. Due to the suppression of the triple higgs self coupling, one can see that the first two diagrams dominate the cross section depending on the effective vertices that are defined by the HEL model. At this point, together with the previous constraints in the literature, we considered the following restrictions to related Wilson coefficients during the signal production:

(1) \bar{c}_B and \bar{c}_W are suppressed, since they should be order of m_W^2/M^2 where M is the typical mass scale of the new physics sector. [14]

(2) \bar{c}_6 is also suppressed for our case, since the corresponding production cross section gives no events at FCC-he.



(a)



(b)

Figure 2: NC signal cross section values over scanned (a) \bar{c}_H (while $\bar{c}_\gamma = 0.1$) and (b) \bar{c}_γ (while $\bar{c}_H = 0.1$) coefficient for $hhZZ$ vertex coupling through $e^-p \rightarrow hhje^-$ process.

(3) Constraints from the electroweak precision parameters suggest that $\bar{c}_T, \bar{c}_W, \bar{c}_B$ should be order of 10^{-3} according to [22].

(4) \bar{c}_W has constrained between $[-1.71, 0.42]$ according to Ref [14] extracted from ATLAS

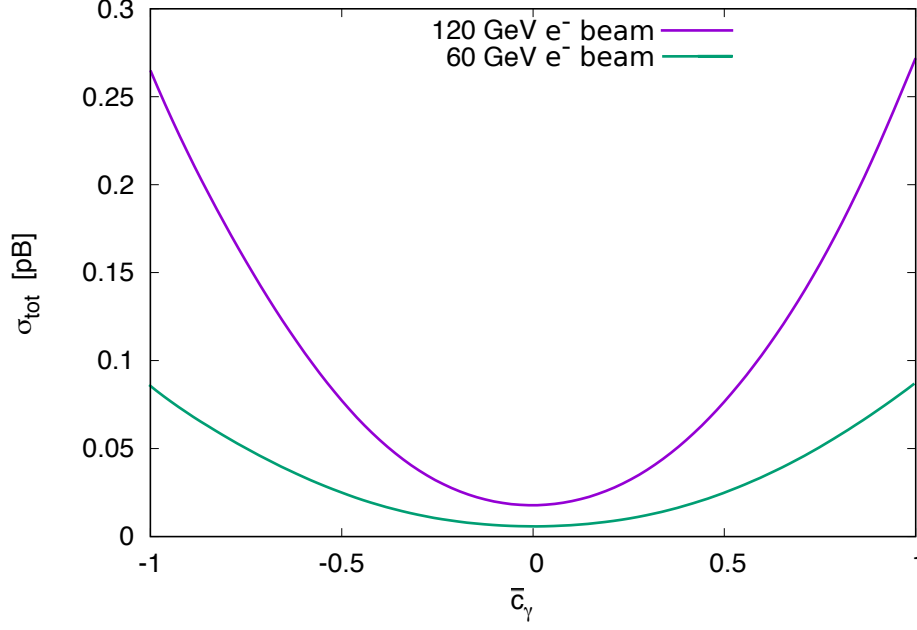


Figure 3: PF signal cross section values over scanned \bar{c}_γ coefficient for $hh\gamma\gamma$ vertex coupling through $e^-p \rightarrow hhje^-$ process.

results [23].

(5) \bar{c}_{HW} and \bar{c}_{HB} that are expected to be order of 10^{-3} tend to cancel each other at the Z-pole.

We investigated $e^-p \rightarrow hhje^-$ process both for Z boson and γ as mediators for the electron polarization: 0 and -0.8. It is considered that the main decay channel of higgs as $h \rightarrow b\bar{b}$ and looked for 4b-jets + Singlejet + lepton in the final state. Note that for PF signal production, we accept $\bar{c}_T, \bar{c}_W, \bar{c}_B = 10^{-3}$ while all other Wilson coefficients are set to zero except scan parameter \bar{c}_γ . Similarly, for VBF signal production, we accept $\bar{c}_T, \bar{c}_W, \bar{c}_B = 10^{-3}$ setting all other Wilson coefficients to zero except scan parameter \bar{c}_H . Thus, two signals, VBF and PF are simulated for negative and positive values of coefficients \bar{c}_H and \bar{c}_γ , respectively. Event data has hadronized by Pythia-PGS [24] and detector level simulation performed by Delphes (version 3.4.1) [25] that are the packages placed in the MadGraph5_aMC@NLO [26] framework 2.5.2 release. Recently announced Delphes baseline detector definitions for FCC-hh have been used to handle the events data by simulation. For detector definitions, particle propagator defined with 1.5 m radius, 5 m half length magnetic field coverage and 4 T z-magnetic field. We assume that the pile-up effects are negligible at both energy and luminosity options of FCC-he collider. Jets are clustered with anti-kT clustering algorithm [27] with a size parameter of $\Delta R = 0.5$ by using FastJet package [28].

From Fig.2 and 3, one can see that a cross section scan over \bar{c}_H , \bar{c}_γ parameters for the processes where $hhZZ$ and $hh\gamma\gamma$ vertices involved. It is trivial that PF signal has higher cross sections if the Wilson coefficient is around $\bar{c}_\gamma \approx 1$. On the other hand, $hhZZ$ vertex has an asymmetric large sensitivity to \bar{c}_γ coefficient as shown in Fig.2b. In Table 3, we present the event counts for signal and background processes where both VBF and PF signals are independently produced.

IV. BACKGROUND PRODUCTION

Although it is highly suppressed in the phase space, one can produce events for $e^-p \rightarrow 2(b\bar{b})je^-$ process in the final state where $j = u(\bar{u}), d(\bar{d}), c(\bar{c}), s(\bar{s}), b(\bar{b})$ quarks within the SM. We calculated the total background cross section to be around $4.5 \times 10^{-5} pb$ for $\sqrt{s} \approx 3.5 TeV$ and $12.5 \times 10^{-5} pb$ for $\sqrt{s} \approx 5 TeV$ energy options. Dominant background contribution in SM is obtained from the tree level multi-jets + lepton productions where we have 4 *b-jets* tagged in the final state. Second main contribution is obtained by $t\bar{t} + 1jet + 1 lepton$ where QCD interactions play important role as well. Inclusively produced two top quarks decay to $W\pm b(b\bar{b})$ and W bosons decay hadronically giving at least 2 *b-jets*, one can obtain ≥ 4 *b-jets* in the final state. Similarly, we have added the contributions of $t(\bar{t})W^{-(+)} + 1jet + 1 lepton$ and $W^{+(-)}W^{-(+)} + 1jet + 1 lepton$ processes in the same investigation and entitled all of these as “All Top & W Inclusive” in Table 3. Third contribution is obtained by electroweak neutral productions such as $ZZ / ZH + 1jet + 1 lepton$ as shown in Table 3. Due to the basic transverse momentum cut applied at 20 GeV for low-pt jets, gluon jets and a small portion of quark jets have been removed. Both signal and background events are produced by setting the factorization and renormalization scales at 125 GeV with standard NN23LO1 parton distribution function set. In productions, *b*-tagging efficiency is assumed to be %60 and considered 1% of light-jets faking the leptons while for *c*-quark jets, the same fake rate is %10.

V. EVENT SELECTION AND ANALYSIS

Event selection criteria: (1) Four *b*-tagged jets and a light jet is selected with $p_T > 20 GeV$. (2) $|\eta| < 5$ for all jets and $|\eta| < 2.5$ for leptons applied. (3) Between jets and *b*-jet and a

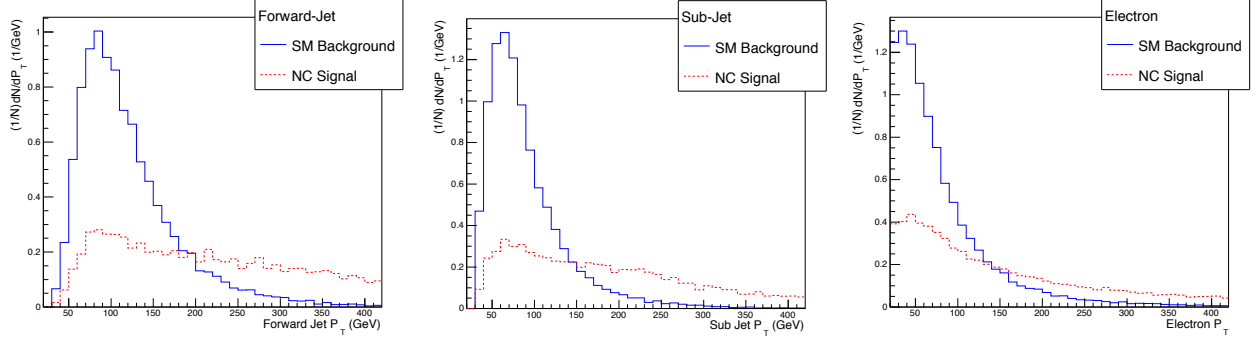


Figure 4: Transverse momentum of forward and sub jets for SM background (blue) and signal (red) respectively.

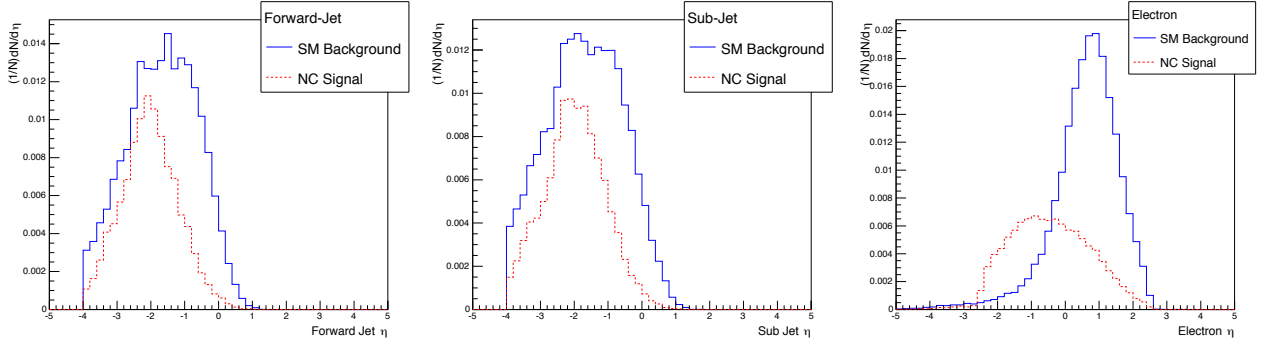


Figure 5: Pseudo-rapidity distributions of leading jet, sub-leading jet and electron for SM background (blue) and signal (red) respectively.

lepton $\Delta R = 0.4$ applied. (4) Event selection cut: $p_T > 150 \text{ GeV}$ for leading jet $p_T > 110 \text{ GeV}$ for sub jets. (5) Invariant mass window cut for both b-jet pairs: $m_{bb} \in [50, 130]$. (6) Vetoing events if missing transverse energy, $E_T > 20 \text{ GeV}$.

In Fig.4 and 5, we present the kinematic distributions in comparison with background and SM processes through a Z boson mediator while $c_H = 0.1$. Fig. 4 shows that the forward and sub jets in signal have a separable transverse momentum than the background jets as expected, while the pseudo-rapidity distributions (Fig.5) behave similar for both signal and background jets. For outgoing electron, one can see that the signal distribution slightly deviates to the negative region, while background signal locates at zero pseudo-rapidity. For the higher values of \bar{c}_H (or \bar{c}_γ in PF process), the higher negative deviation for the mean of pseudo-rapidity distributions are observed. In Fig.6, it is seen the reconstructed invariant mass distribution of one Higgs boson (M_H) from two b-jets within di-Higgs for both signal and background located at around 125 GeV. This also shows that in SM, the large

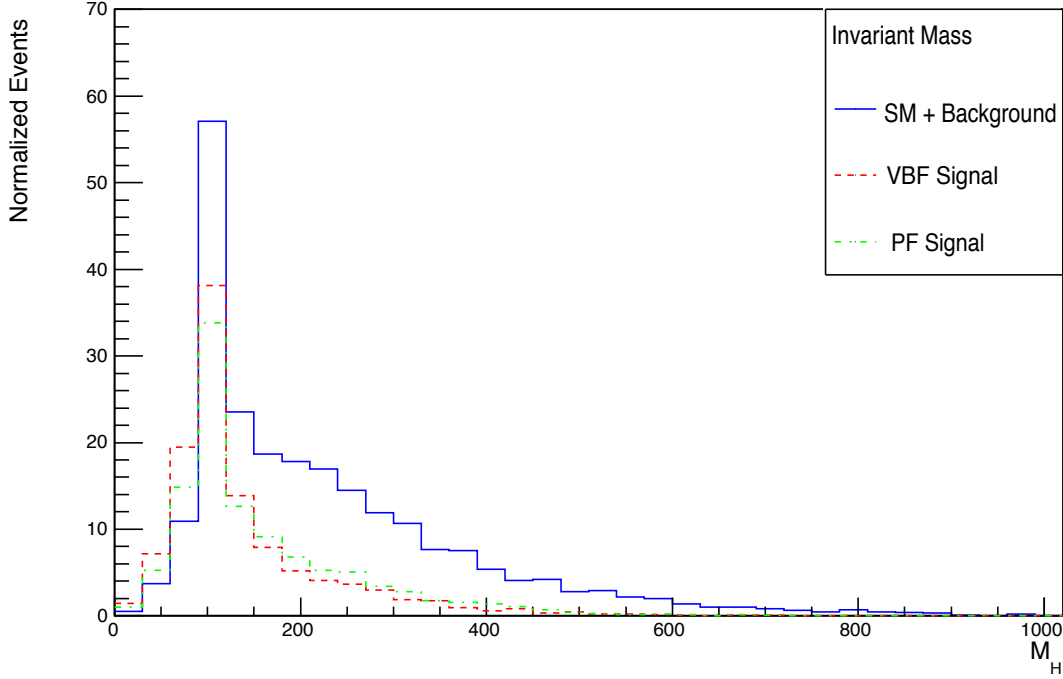


Figure 6: Reconstructed invariant mass distribution of Higgs from two b-jets for SM background (blue), VBF signal (red) and PF signal (green).

contribution comes from the b-jets created by di-Higgs decays. As a significant evidence for coupling separations, azimuthal angle distribution ($\Delta\phi$) between lepton and forward jet for VBF and PF signals are shown in Fig.7 and Fig.8, respectively for $\sqrt{s} \approx 5 \text{ TeV}$. Similarly for $\sqrt{s} \approx 3.5 \text{ TeV}$, same distributions are observed with a factor ~ 0.286 in the event count. About the shape of the distribution of $\Delta\phi$, we observed that this interference is strictly dependent on the coefficients and detector parameters. For evaluating the limits in Fig.9, we calculated statistical significances and followed the methods described in Ref.[29] It's also worthwhile to comment on the event selection criteria: First three conditions consist of almost default cuts for event production. Fourth condition has higher p_T cuts that can be seen directly from Fig.4 to separate signal from background. Fifth condition is extremely effective if b-jets are not produced by a higgs decay. Sixth condition is also an important selection criteria especially for removing top background since W^+/W^- bosons from a top quark decay emerge neutrinos while decaying to leptons. For hadronic decay of W bosons, note that $Br(W^-/W^+ \rightarrow \bar{c}b/c\bar{b}) \sim 0.01$ leaves fairly less b-pairs in the final state. We have determined cuts after obtained kinematic distributions as Fig.4-6 and optimised scanning

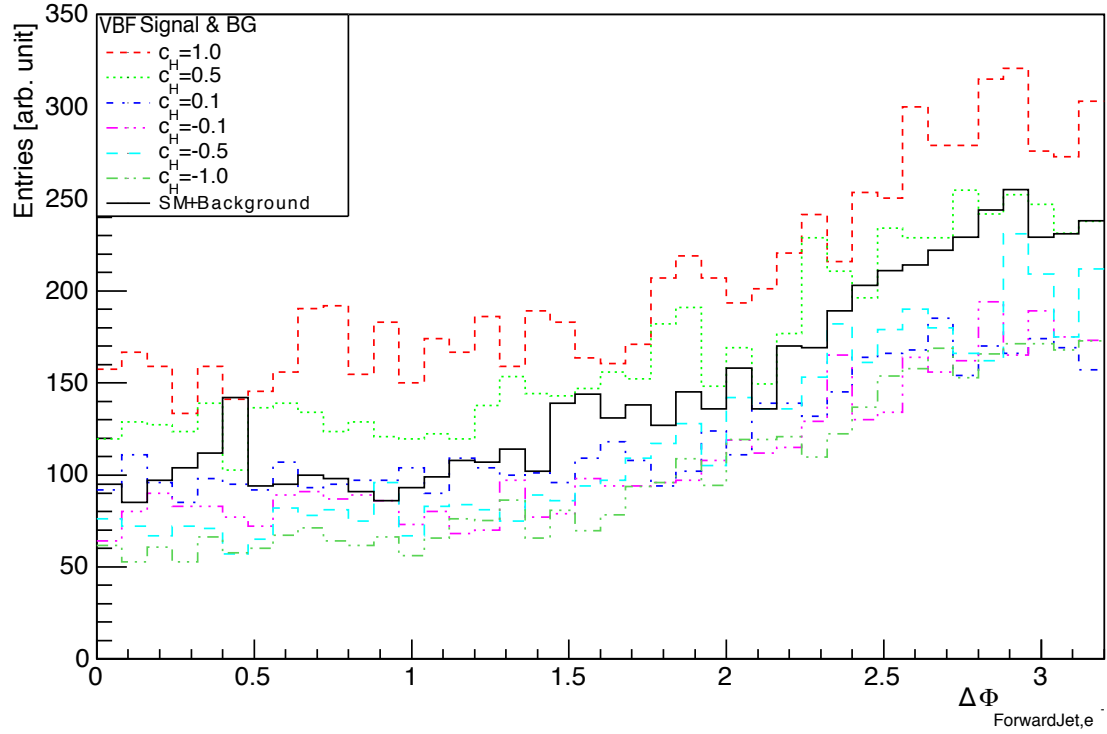


Figure 7: Azimuthal angle distribution of lepton and forward jet of VBF signal for $\bar{c}_H = \pm 0.1, \pm 0.5, \pm 1$ with SM + background (black) for $\sqrt{s} \approx 5 \text{ TeV}$ option.

over variables to obtain the highest significance, namely $\frac{S}{\sqrt{B}}$ where S signal events and B background events. The last two columns of Table 3, denote the survived event numbers after applying our selection criteria.

To evaluate above predictions within the realistic perspective, one should consider reconstruction efficiencies from the detector, systematic errors on luminosity measurements and pile-up treating. Note that along with the b-tagging efficiency, W/Z reconstruction efficiencies and uncertainties in decay channels may affect sensitivity results as mentioned for LHC in Ref [30]. These uncertainties which are obtained directly from previous experiments, will likely to improve with integrated luminosity. For ease of comparison, while a reduction of total statistical and experimental systematic uncertainties by a factor of about 0.3 for $L_{int} = 300 \text{ fb}^{-1}$ and about 0.1 for $L_{int} = 3000 \text{ fb}^{-1}$ for LHC, one should expect a lower factor extrapolating the same idea for FCC-he.

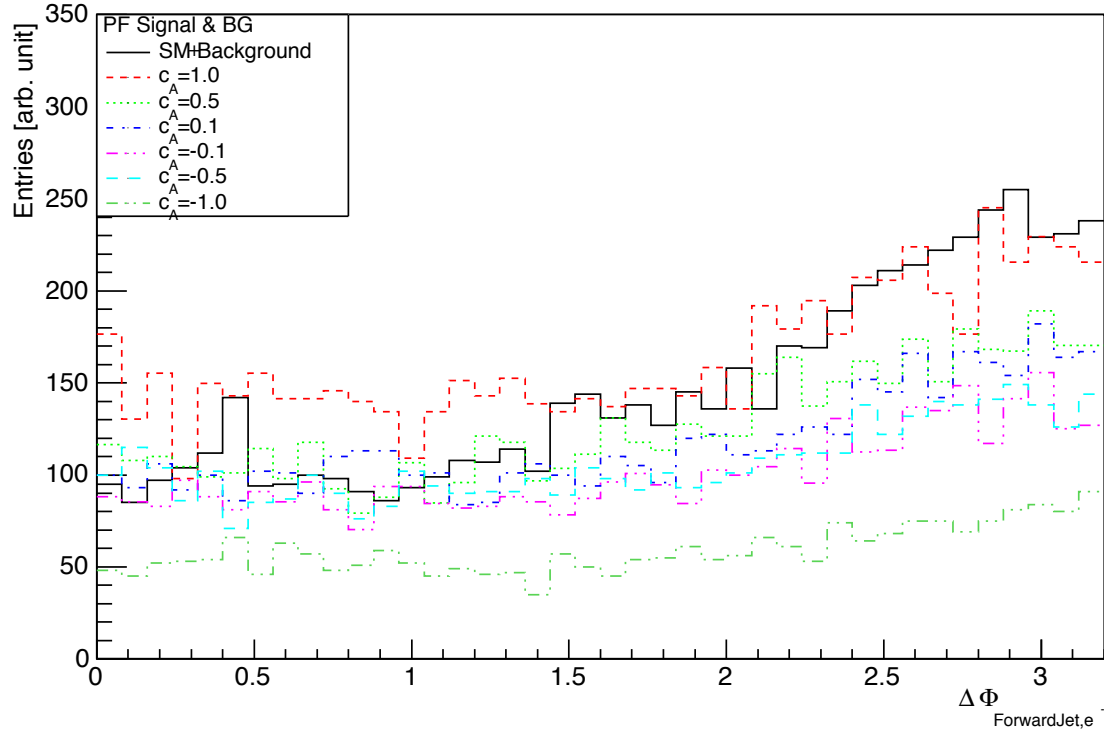


Figure 8: Azimuthal angle distribution of lepton and forward jet of PF signal for $\bar{c}_\gamma = \pm 0.1, \pm 0.5, \pm 1$ with SM + background (black) for $\sqrt{s} \approx 5 \text{ TeV}$ option.

VI. CONCLUSION

In this letter, we have investigated the sensitivity on the Higgs boson couplings and Wilson coefficients in productions through NC mechanism (in Fig. 1) for FCC-he. Since the process is possible through both Z boson and γ mediators, one should take into account the interference of VBF and PF processes with the right parameter set. We observed that $\Delta\phi$ variable which is strictly affected by detector parameters, is a key to separate interferences of both VBF and PF signals. It is observed that di-Higgs production through NC mechanism has a major sensitivity to \bar{c}_γ and \bar{c}_H coefficients within the considerations of electroweak precision measurements. FCC-he collider can cover $\bar{c}_H(\bar{c}_\gamma)$ coefficients as in Fig.9 through NC processes with integrated luminosities up to 3 (50) ab^{-1} respectively. On the other hand, one can reveal the corresponding Higgs couplings by obtaining limits of Wilson parametrization that is involved in Higgs productions at a specific limunosity. Thus, we present $g_{hh\gamma\gamma}/\tilde{g}_{hh\gamma\gamma}$, g_{hhzz} and \tilde{g}_{hhzz} in Fig. 10 that shows the required limunosities to discover these couplings.

Table III: Signal and Background events for $\mathcal{L}_{int} = 10 \text{ ab}^{-1}$

		$\sqrt{s} \approx 3.5 \text{ TeV}$	$\sqrt{s} \approx 5 \text{ TeV}$	$\sqrt{s} \approx 3.5 \text{ TeV}(\text{with cuts})$	$\sqrt{s} \approx 5 \text{ TeV} (\text{with cuts})$
VBF Signal:	$c_H = 1.0$	1333	3493	224	668
	$c_H = 0.5$	493	1383	102	352
	$c_H = 0.1$	169	561	55	213
PF Signal:	$c_\gamma = 1.0$	876803	2571242	428204	1496202
	$c_\gamma = 0.5$	22471	712902	10544	384701
	$c_\gamma = 0.1$	8651	26921	4353	15764
[Backgrounds]					
4 bjets + 1 jet + 1 e-		120343	258911	2	11
All Top & W Inclusive		82787	216209	349	975
Z / H + 2bjets + 1 jet + 1 e-		1634.2	38264	22	89
Z / ZZ + 1 jet + 1 e-		1625.4	2760	55	116
ZH + 1 jet + 1 e-		407	690	24	58
Total Background		206796.6	516834	452	1249
$\frac{S}{\sqrt{B}}$ for VBF				10.5	18.9
				4.8	9.96
				2.58	6.03
$\frac{S}{\sqrt{B}}$ for PF				2×10^4	4.2×10^4
				496	10^4
				204	446

An integrated luminosity of 10 ab^{-1} can set limits on these couplings $[-0.0005, 0.0005]$, $[-0.05, 0.05]$ and $[-0.012, 0.012]$ respectively. Although our approach is based on the single parameter dominance hypothesis, considering the Wilson coefficients, one can compare the \bar{c}_H (\bar{c}_γ) constraints obtained by LHC data in Ref [30]. It is seen that LHC (with $L_{int} = 3000 \text{ fb}^{-1}$) targeted to set similar limits on compared coefficients \bar{c}_H (\bar{c}_γ) with the FCC-he collider at the same luminosity levels. However, this comparison of different types of colliders should be made in the context of uncertainties and systematic errors on which FCC-he may have some advantages as a future collider.

For EFT approach, it is known that above the new physics scale, Λ , Lagrangian expansions will be unconvinced and limits on the couplings will deteriorate rapidly. One can see from the Wilson parametrization that the coefficients can naively be expressed in terms of M,

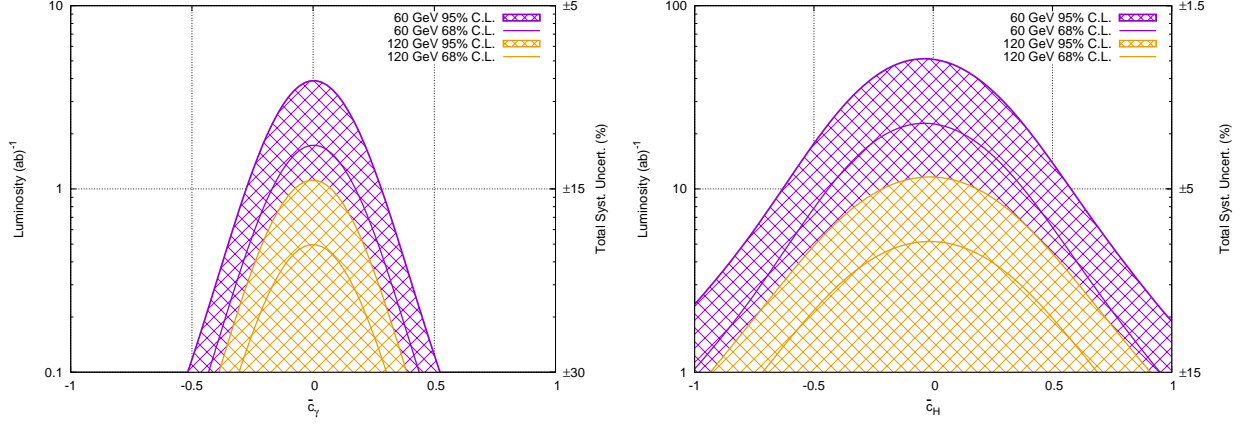


Figure 9: Required integrated luminosities to obtain the limits on Wilson coefficients \bar{c}_H , \bar{c}_γ for 60 GeV and 120 GeV electron beam energy options at FCC-he where the shaded areas are not allowed assuming $\bar{c}_T, \bar{c}_W, \bar{c}_B = 10^{-3}$ and all other Wilson coefficients are zero. Total systematic uncertainties are roughly extrapolated from LHC data in percentage.

overall mass scale. However, couplings such as $\tilde{g}_{hh\gamma\gamma}$, \tilde{g}_{hhzz} that have degrading sensitivities because of the higher order dependences, have deterioration of limits such that, at higher energies, deviations from the original limit in percentage getting lower. Thus, according to recent mass limits on heavy particles, one can see that the deterioration of limits cannot deviate above %10. Although similar detailed searches at the LHC are available to set limits on corresponding Higgs couplings, it is possible to obtain high precision on the couplings using FCC-he advantages in center of mass energy and background.

ACKNOWLEDGEMENT

We would like to thank especially Dr. Uta Klein, Dr. Bruce Mellado, Dr. Rob Apsimon and Dr. Orhan Cakir for their comments, fruitful discussions for this work.

-
- [1] Higgs, P. (1964). Broken symmetries and the masses of gauge bosons. Phys. Rev. Lett. 13, 508–509.
 - [2] Englert, F. & Brout, R. (1964). Broken symmetry and the mass of gauge vector mesons. Phys. Rev. Lett. 13, 321–323.
 - [3] Aad, G. et al. (2012). [ATLAS Collaboration], Phys. Lett. B 716, 1.
 - [4] Chatrchyan, S. et al. (2012). [CMS Collaboration], Phys. Lett. B 716, 30.

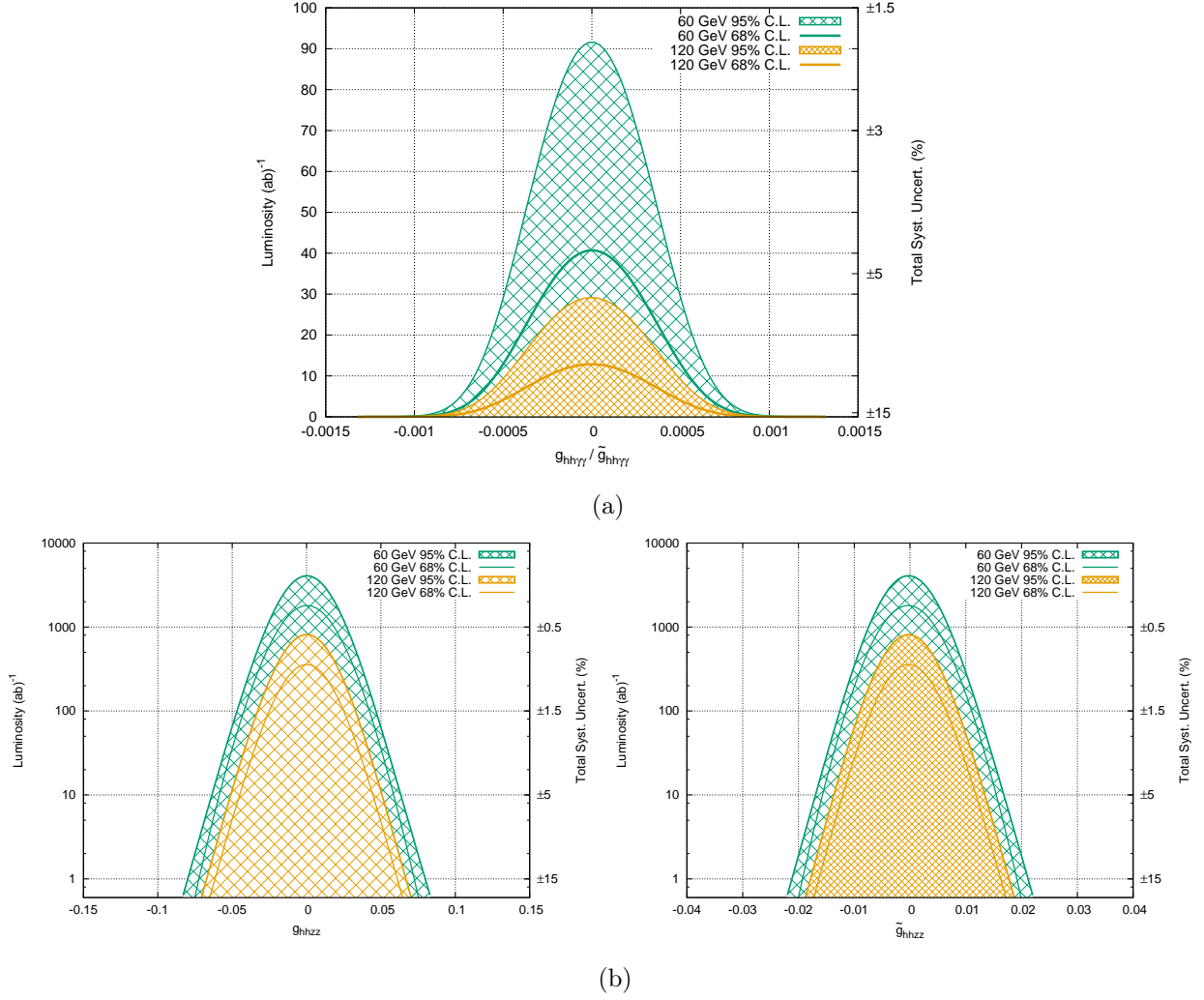


Figure 10: Required integrated luminosities to obtain the limits on the corresponding couplings (a) $g_{hh\gamma\gamma}/\tilde{g}_{hh\gamma\gamma}$ (b) g_{hhzz} and \tilde{g}_{hhzz} for 60 GeV and 120 GeV electron beam energy options at FCC-he where the shaded areas are not allowed assuming $\bar{c}_T, \bar{c}_W, \bar{c}_B = 10^{-3}$ and all other Wilson coefficients are zero. Total systematic uncertainties are roughly extrapolated from LHC data in percentage.

- [5] Pich, A. (2016). Electroweak Symmetry Breaking and the Higgs Boson, Acta Phys. Polon. B 47 151 [arXiv:1512.08749].
- [6] Spira, M. Djouadi, A. Graudenz, D. Zerwas, P.M. (1995) Higgs boson production at the LHC Phenomenology-HEP Nucl.Phys. B453 17-82. [arXiv:hep-ph/9504378].
- [7] Bolzoni, P., Maltoni, F., Moch, S., Zaro, M. (2010). Higgs production via vector-boson fusion at NNLO in QCD, Phys.Rev.Lett. 105 011801 arXiv:1003.4451 [hep-ph] DESY-10-042, SFB-CPP-10-23, CP3-10-12.

- [8] Gay, A. (2007) Measurement of the top-Higgs Yukawa coupling at a linear e^+e^- collider, Eur. Phys. J. C 49: 489. [arXiv:hep-ph/0604034].
- [9] Han, T., Mellado, B. (2010). Higgs boson searches and the $H\bar{b}b$ coupling at the LHeC, Phys. Rev. D 82, 016009.
- [10] d’Enterria, D. (2017). Higgs physics at the Future Circular Collider, [arXiv:1701.02663].
- [11] Kumar, M. et al. (2017) Probing anomalous couplings using di-Higgs production in electron–proton collisions, Physics Letters B, Volume 764, 10 January 2017, Pages 247-253. [arXiv:1509.04016].
- [12] Khanpour, H. et al. (2017) Constraining Higgs boson effective couplings at electron-positron colliders, Phys. Rev. D 95, 055026, [arXiv:1702.00951]
- [13] Khanpour, H. et al. (2017) Probing Higgs boson couplings in $H+\gamma$ production at the LHC, Physics Letters B, Volume 773, 2017, Pages 462-469, [arXiv:1702.05753]
- [14] Alloul, A., Fuks, B. & Sanz, V. (2014). Phenomenology of the Higgs Effective Lagrangian via FeynRules, J. High Energ. Phys. 2014: 110.
- [15] von Buddenbrock, S., Chakrabarty, N., Cornell, A.S. et al. Eur. Phys. J. C (2016) 76: 580. doi:10.1140/epjc/s10052-016-4435-8.
- [16] von Buddenbrock, S., Chakrabarty, N., Cornell, A.S. et al., (2015) The compatibility of LHC Run 1 data with a heavy scalar of mass around 270 GeV, [arXiv:1506.00612v2].
- [17] Artoisenet, P., de Aquino, P., Demartin, F., Frederix, R., Frixione, S. et al. (2013). A framework for Higgs characterisation, JHEP 11 043 [arXiv:1306.6464].
- [18] G. Giudice, C. Grojean, A. Pomarol, and R. Rattazzi, The Strongly-Interacting Light Higgs, JHEP 0706 (2007) 045, [hep-ph/0703164].
- [19] Contino, R., Ghezzi, M., Grojean, C., Muhlleitner, M. and Spira, M. (2013) Effective Lagrangian for a light Higgs-like scalar, JHEP 07 (2013) 035 [arXiv:1303.3876].
- [20] <https://feynrules.irmp.ucl.ac.be/wiki/HEL>
- [21] <https://feynrules.irmp.ucl.ac.be>
- [22] M. Baak, M. Goebel, J. Haller, A. Hoecker, D. Kennedy et al., The Electroweak Fit of the Standard Model after the Discovery of a New Boson at the LHC, Eur. Phys. J. C 72 (2012) 2205 [arXiv:1209.2716].
- [23] ATLAS Collaboration, Measurements of Higgs boson production and couplings in diboson final states with the ATLAS detector at the LHC, Phys. Lett. B 726 (2013) 88 [arXiv:1307.1427].

- [24] Sjostrand, T., Mrenna, S. and Skands, P.Z. (2006) JHEP 0605, 026.
- [25] de Favereau, J. et al. (2014) [DELPHES 3 Collaboration], JHEP 1402, 057.
- [26] Alwall, J., Frederix, R., Frixione, S. et al. J. High Energ. Phys. (2014) 2014: 79. doi:10.1007/JHEP07(2014)079 [arXiv:1405.0301].
- [27] M. Cacciari, G. P. Salam, and G. Soyez, “The anti-kt jet clustering algorithm”, JHEP 04 (2008) 063, doi:10.1088/1126-6708/2008/04/063, arXiv:0802.1189.
- [28] M. Cacciari, G.P. Salam and G. Soyez, “FastJet User Manual”, Eur.Phys.J. C72 (2012) 1896, doi: 10.1140/epjc/s10052-012-1896-2, [arXiv:1111.6097].
- [29] Cowan, G., Cranmer, K., Gross, E. et al. Eur. Phys. J. C (2011) 71. 1554. doi:10.1140/epjc/s10052-011-1554-0 [arXiv:1007.1727v3].
- [30] Englert, C., Kogler, R., Schulz, H. et al. Eur. Phys. J. C (2016) 76: 393. [arXiv:1511.05170].